Mechanical Systems and Signal Processing 196 (2023) 110333

Contents lists available at ScienceDirect

Mechanical Systems and Signal Processing

journal homepage: www.elsevier.com/locate/ymssp

# A novel DISTINCT method for characterizing breathing features of nonlinear damage in structures

Qingyang Wei [a], Maosen Cao [e,d,*], Lei Shen [b], Xiangdong Qian [a], László Dunai [c,d], Wiesław Ostachowicz [f]

[a] College of Mechanics and Materials, Hohai University, Nanjing, China
[b] College of Water Conservancy and Hydropower Engineering, Hohai University, Nanjing, China
[c] Department of Structural Engineering, Budapest University of Technology and Economics, Budapest, Hungary
[d] Jiangxi Province Key Laboratory of Environmental Geotechnical Engineering and Hazards Control, Jiangxi University of Science and Technology, Ganzhou, China
[e] Institute of Structural Dynamics and Control, Hohai University, Nanjing, China
[f] Institute of Fluid-Flow Machinery, Polish Academy of Sciences, Gdansk, Poland

A R T I C L E I N F O

Communicated by: Paulo Kurka

*Keywords:*
Breathing crack
Nonlinear feature
Super harmonics
Inherent nonlinearity
Arch dam
Seismic testing

A B S T R A C T

The detection of breathing cracks in in-service structures is an intractable issue due to the distinctive dynamic behavior, typically the opening and closing of the crack subjected to cyclic loading. The existing methods to identify breathing cracks generally rely on the hypothesis of the crack-induced nonlinear features, mostly represented by super-harmonics. Nevertheless, an in-service structure even free of cracking somehow has nonlinear components in material, geometry, boundary etc., such that it tends to present inherent nonlinear features, i.e., nonlinearities prior to cracking, which could impair the effectiveness of super harmonics-like methods to depict breathing cracks. In such a circumstance, a sophisticated method that can characterize breathing cracks-induced nonlinearity by accommodating inherent nonlinear of the structure is desired. Herein, a novel method, termed DISTINCT (Difference in Split Temporal signal with Inherent Nonlinear Components Tolerated) method, is proposed. This method is formulated by splitting a whole response of a structure bearing breathing cracks into positive and negative response components. Each response component largely reflects structural dynamic behavior with regard to the crack-opening state or crack-closing state. From positive or negative response components, the dynamic property such as the frequency spectrum arising from the Fast Fourier Transform, corresponding to crack-opening state or crack-closing state, can be derived. To this end, the differences between the two frequency spectra relatively purely manifests the characteristic of breathing cracks including their presence and severity. The feasibility of the DISTINCT method is numerically verified via the identification of breathing crack in a cantilever beam and a shell, with emphasis on its stronger noise resistance than the traditional super-harmonics-based method. Furthermore, the method's effectiveness is experimentally validated via the inspection of breathing cracks in a scaled arch dam model subject to excitations induced by artificial seismic accelerations. The results show that the proposed DISTINCT method can quantify the severities of four levels of damage comprising breathing cracks by tolerating inherent nonlinearity of the structure. The advantages of the DISTINCT lie in its tolerance to structural inherent nonlinearities

* Corresponding author.
*E-mail address:* cmszhy@hhu.edu.cn (M. Cao).

https://doi.org/10.1016/j.ymssp.2023.110333
Received 6 October 2022; Received in revised form 27 January 2023; Accepted 27 March 2023
Available online 17 April 2023

and requiring no numerical or physical benchmarks nor any prior knowledge of the material properties and boundary conditions in assessing breathing cracks of structures.

## 1. Introduction

Cracks tend to germinate and propagate in structures under cyclic loading, which endangers the integrity and safety of structures. The existing cracks, if not detected and repaired, may eventually cause disastrous effects as the severity of cracks increases [1]. Non-destructive testing equipments and methods are usually applied to detect the presence, location, and severity of cracks so as to take necessary maintenance, repair, and retrofit actions [2]. Traditional non-destructive detections are usually based on acoustic emission inspection, film radiography, magnetic particle inspection, and ultrasonic wave propagation. Unfortunately, these methods have deficiencies such as high cost, complicated operational procedure, and applicability to limited specific scenarios [3]. Alternatively, the vibration-based methods provide dissimilar ways of crack identification and have largely captured the interest of academics in recent years due to their high effectiveness and efficiency [4,5]. Besides, vibration-based methods supply more possibilities for online monitoring without interfering with regular operation [6,7].

The early vibration-based crack detection methods primarily concentrated on the differences in modal parameters between the intact and cracked structures [8,9]. Frequency reduction and damping increase represent the propagation of crack [10–12]. The singularity of the vibration mode contains the crack location information [13]. Meanwhile, more detection methods such as the frequency response function, flexibility matrix, substructure identification and other vibration information have been developed with more damage indicators proposed [14–17]. Nevertheless, these methods are appealing to linear damage, exposing shortcomings in identifying practical damage that has a nonlinear feature [18,19]. Researchers have reached the common opinion that of the presence of cracks causes structures to have nonlinear features rather than always exhibiting linear behavior [20]. Especially, fatigue cracks tend to open and close under cyclic loading, known as the "breathing effect" [21]. Yang et al. [22,23] presented four types of detection indicators for rotating blades with the proposed high-fidelity breathing crack model for rotating blades by investigating the vibration responses. Nguyen [24] presented a wavelet spectrum technique to determine the presence of breathing cracks by the change of instantaneous frequency during vibration. Wimarshana et al. [25] experimentally realized using entropy measures to distinguishing the depths of the breathing crack in a beam.

Regarding the detection of breathing cracks, a more recent research trend involves using the nonlinear features of the free or forced response of structures [26–28]. Neild et al. [29] experimentally explored the cracks in reinforced concrete beams by nonlinear index, i.e., the frequency exhibits correlation with the vibration amplitude. Time-frequency analysis was used by Wang et al. [30] to derive the curves of displacement amplitudes corresponding to vibration frequencies; the method was shown to be effective for structures with small invisible cracks. Chen et al. [31] proposed a nonlinear damage indicator for the detection of newly induced damage in a reinforced concrete flexural member based on two frequency response functions; the frequency response functions obtained by the forward and reverse sweep frequency excitation are skewed to the lower frequency side as the severity of damage increases. Andreaus and Baragatti [32] applied super-harmonic components and the relative amplitude with respect to the fundamental frequency as a damage indicator, which was able to determine the presence of damage in the structure and to approximately estimate the relative importance of the damage itself. Giannini et al. [21] numerically investigated the relation between the harmonic component amplitude and damage characteristics of a cantilever beam forced by harmonic excitation at the free end. Lu et al. [33] proposed a model updating based method for identifying the breathing crack of rotors by using the super-harmonic nonlinear characteristics. Yang et al. [34] verified the super-harmonic resonances can serve as a distinguishable indicators for diagnosing the crack existence and the third-order super-harmonic resonances can serve as an indicator for the presence of severe crack. Wang et al. [35] applied two damage indicators including distortion value of phase spectrum and proportion of super- and sub-harmonic amplitudes to characterize the change of fatigue crack with different damage location and severity. Al-hababi et al. [36] developed a robust nonlinear damage factor using dual Fourier transform for damage detection and quantification of fatigue-breathing cracks in beam-like structures. Yan et al. [37] transferred the bilinear system identification into two linear system identification and combined the Hilbert transform for distinguishing the varied frequencies induced by the breathing crack. Besides, several other nonlinearity-based techniques have been developed in order to detect cracks, using nonlinear approaches such as information on phase diagram geometry [38–40], the Volterra series [41–43] and the higher order spectra analysis [44,45].

Nevertheless, the main issue with these nonlinear methods is that the intact structures exhibit inherent nonlinear features: such as the super-harmonics associated with boundary conditions or excitation devices, and the inherent material nonlinearity of a structure consisting of concrete that causes the frequency dependence on amplitude, which limits or even renders of these methods ineffective [39,46]. Therefore, a detection method named DISTINCT (Difference in Split Temporal signal with Inherent Nonlinear Components Tolerated), which aims to overcome the limitations induced by inherent nonlinearities, is proposed. The method enjoys the merits of characterizing breathing cracks by tolerating the inherent nonlinearity interferences caused by incomplete fixed boundary or nonlinear excitation equipment in the process of forced excitation [47,48]. Such inherent nonlinearities are usually obstacles that incapacitate the super-harmonics-based method in portraying breathing cracks. The method is proposed meanwhile for pursuing the advantages of easy implement in algorithm and hardware, and sensitivity to the damage of breathing cracks. A relatively advanced and widely used existing method based on super-harmonics is compared with the proposed DISTINCT method. This super-harmonics-based method takes the appearance of multiple peaks of excitation frequency in the frequency domain the of breathing-cracked structure evoked by harmonic excitation as the indication of breathing cracks.

The rest of this paper is organized as follows. Section 2 presents the formulation of the proposed DISTINCT method. Section 3 provides numerical verifications for the proposed DISTINCT method by investigating the algorithm effectiveness, characteristics and generalization. Section 4 describes the experimental validation of the proposed DISTINCT method by a shaking test of a scaled arch dam model. Finally, conclusions are presented in Section 5.

## 2. Formulation of DISTINCT method

### 2.1. Method definition

When a structure with a breathing crack is excited by a harmonic force with a frequency equal to the fundamental frequency of the structure, the state of two crack surfaces varies from detachment to compression, i.e., crack opening and crack closing, within one period of vibration. For simplicity, a bilinear function is adopted to simulate the breathing crack that closes when the normal strain of the crack section is negative and that opens when the normal strain of the crack section is positive. In this circumstance, the vibration response of a structure with a breathing crack can be considered to contain two components: positive and negative response components with the $x$-axis as a split line, with respect to states of crack opening and crack closing. The positive and negative response components reflect the vibration characteristics of the breathing-crack structure in the crack-opening and crack-closing states, respectively. The forced vibration response of this bilinear system can be represented as shown in Fig. 1.

The vibration response in Fig. 1 has $N$ vibration periods, each period consisting of the negative vibration response in crack closing state and the positive vibration response in crack opening state. The duration of crack opening and crack closing in each period are denoted by $T_1$ and $T_2$, respectively.

$$T_1 = \frac{1}{2f_o} \tag{1}$$

$$T_2 = \frac{1}{2f_c} \tag{2}$$

where, $f_c$ and $f_o$ are the fundamental frequency of this system in crack closing state and crack opening state, respectively.

The total duration of crack closing state and crack opening state in this response are denoted by $T_{s1}$ and $T_{S2}$, respectively.

$$T_{s1} = T_1 + T_1 + \cdots + T_1 = NT_1 \tag{3}$$

$$T_{s2} = T_2 + T_2 + \cdots + T_2 = NT_2 \tag{4}$$

The total duration of this response is denoted by $T_s$.

$$T_s = N(T_1 + T_2) = \frac{N}{2}\left(\frac{1}{f_c} + \frac{1}{f_o}\right) \tag{5}$$

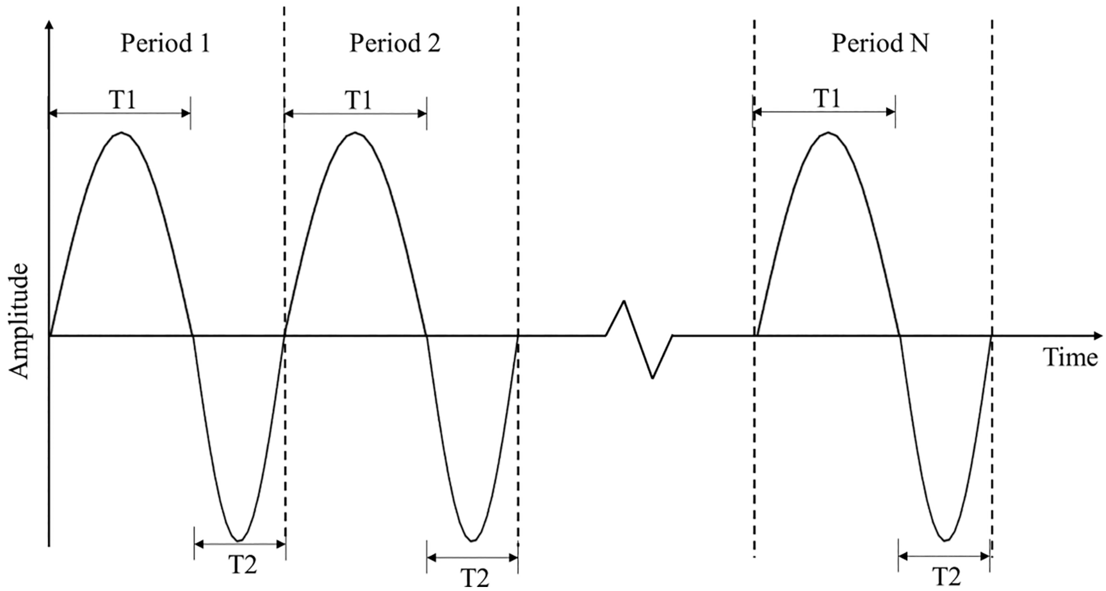


**Fig. 1.** Schematic diagram of forced vibration response of a bilinear system.

The distinction between the two components' frequencies, called $f_c$ and $f_o$, should be made. The frequency of the structure with breathing crack simulated as a bilinear function, so-called breathing-frequency, can be denoted as

$$f_b = \frac{N}{T_s} = 2\frac{f_c f_o}{(f_c + f_o)} \tag{6}$$

The positive and negative response components represent vibration characteristics of the system in the opening and closing states of the crack, respectively, which implies the difference between these two types of responses components can characterize the property of a breathing crack. This idea forms a basic principle of identifying the breathing crack in a structure through inspecting the positive and negative response components produced by splitting a whole response along the $x$-axis on the condition that a breathing crack can be simulated as a bilinear system. Hereinafter, the positive and negative response components are called split components for brevity.

From the principle, the degree of difference between the split response components reflects the severity of breathing cracks; moreover, such a difference can be intuitively investigated by comparing their frequency contents. Specifically, the frequency spectra of the positive and negative components can be evaluated by the Fast Fourier Transform (FFT) and their difference denotes designates the breathing crack. The opening frequency, $f_o$, should be lower than the closing frequency, $f_c$, since the presence of opening reduces the sectional stiffness and the degree of opening is positively correlated with that of reduction in sectional stiffness. The difference between closing and opening frequencies can be expressed as $\Delta f$:

$$\Delta f = f_c - f_o \tag{7}$$

Considering that the positive and negative response components may not be easily distinguished in applications, a damage index is

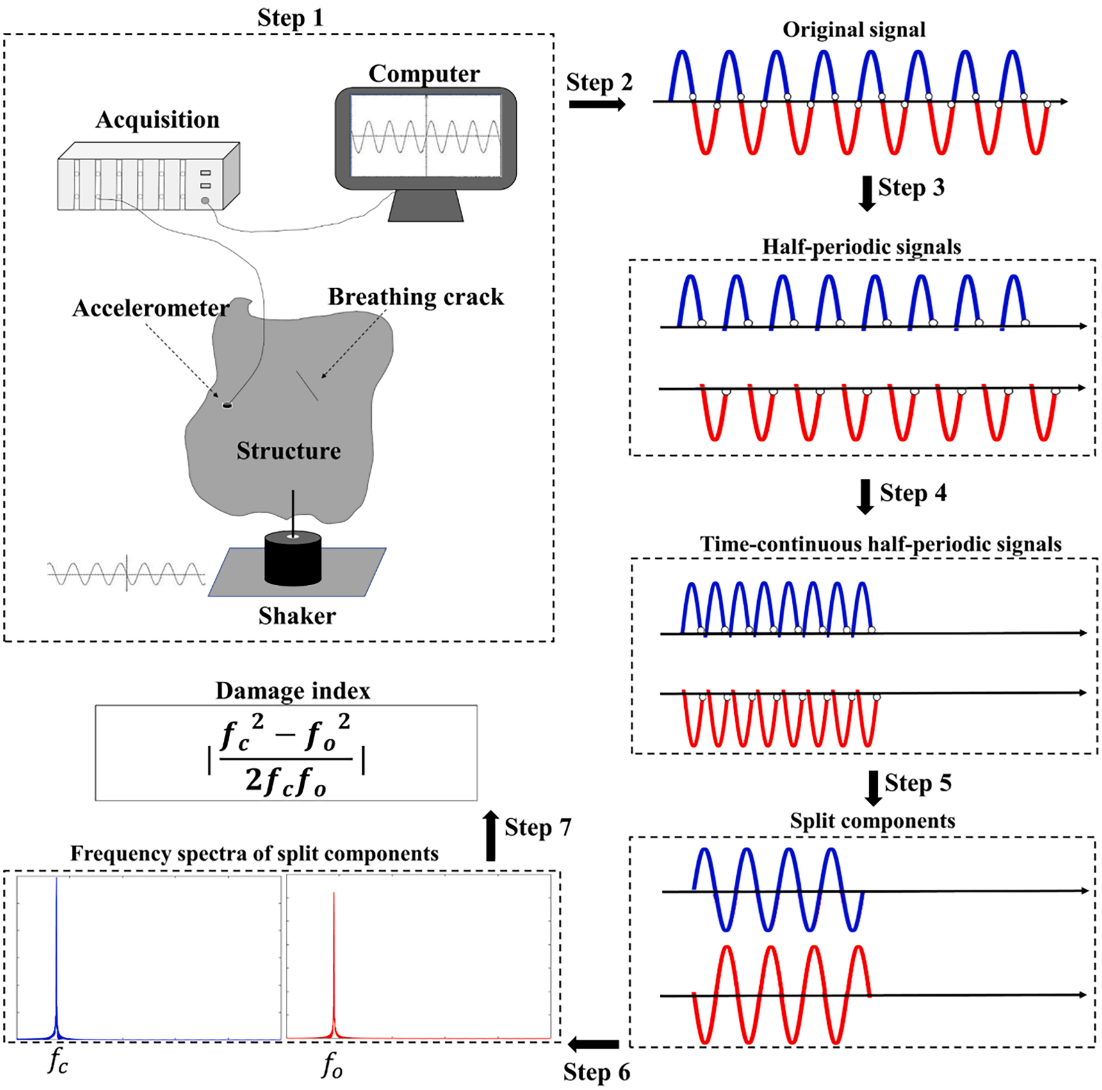


**Fig. 2.** Schematic diagram of the DISTINCT method.

defined as

$$DI = |\frac{\Delta f}{f_b}| = |\frac{f_c^{\ 2} - f_o^{\ 2}}{2 f_c f_o}| \tag{8}$$

This damage index depicts the severity of breathing cracks using the ratio of the frequency difference between the closing and opening frequencies to the breathing frequency. Further, (1) if the structures exhibit material nonlinearity that is mainly affected by vibration amplitude. The harmonic forced vibration at a certain amplitude which the proposed method used will not be affected by the material nonlinearity whereas the free vibration that other methods used can be affected. This approach is hence immune to the inherent material nonlinearity.

(2) if there is inherent nonlinearity caused by the weak region of connection between the exciter and the structure or the exciter itself in the structure. This inherent nonlinearity should be considered as relatively small, appearing in the high frequency part, which is often a multiple of the fundamental frequency, and not having a significant enough impact to interfere with the frequency separation that is the method's core feature.

This method for detecting breathing cracks via avoiding the influences of the differences in environmental conditions and measurement errors before and after cracking, because the frequencies of the split components are extracted by splitting the same whole responses measured in the current state. More importantly, this method is immune to different initial nonlinearities caused by non-damage factors. In addition, this method has the advantage of not requiring the baseline information about the structure, i.e., the frequency of the intact structure.

### *2.2. Method implementation*

The procedure of DISTINCT method involving seven steps is schematically represented in Fig. 2. This figure offers a brief profile of using the DISTINCT method to identify breathing cracks step by step with each step interpreted as follows.

Step 1: Set up excitation devices, sensors, harmonic excitation frequency, with which the vibration response $x(i)$ to the harmonic excitation is collected.
Step 2: Track the zero crossings of $x(i)$ in sequence. Each zero crossing is bounded by an upper zero-point and a lower zero-point, specified with $x(i) \geq 0\&x(i+1)\langle 0$, and $x(i) \leq 0\&x(i+1)\rangle 0$, respectively.
Step 3: Split the original signal into two half-periodic signals: one with positive response value and the other with negative response value by using upper and lower zero-points. The upper and lower zero-points themselves are included in the half-periodic signal with positive response value and the half-periodic signal with negative response value.
Step 4: Eliminate the time interval after splitting in the half-periodic signals and then define the eliminated signals as time-continuous half-periodic signals. The first value after any half-periodic response is followed by the first value of the subsequent half-periodic response during the elimination process.

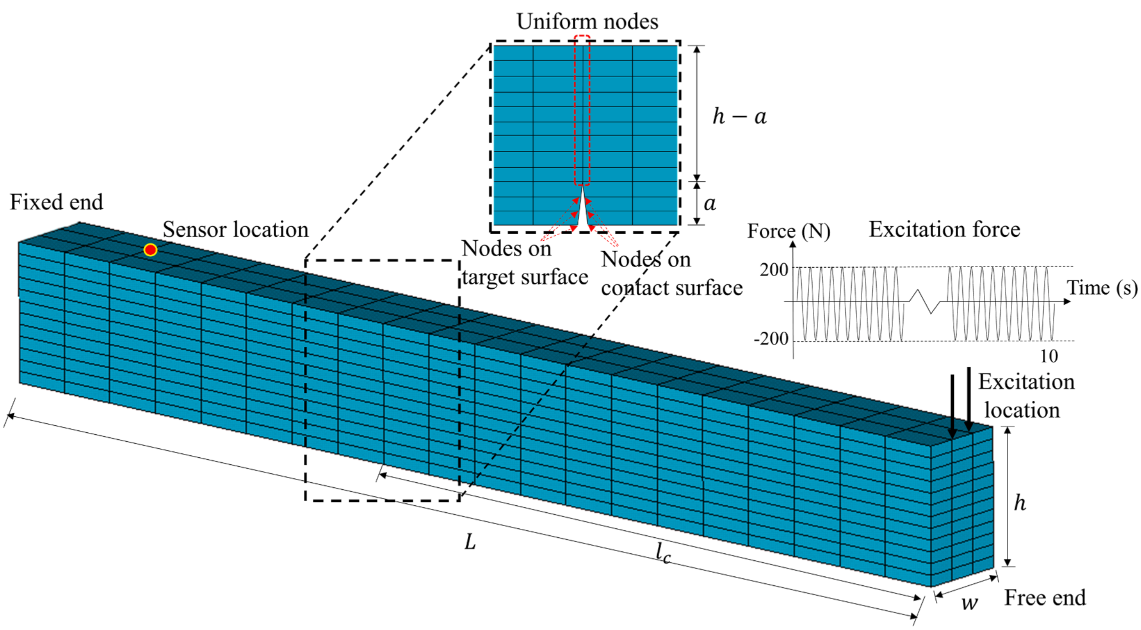


**Fig. 3.** Finite element model of a breathing-cracked cantilever beam.

Step 5: Flip the odd or even number order half-periodic responses of all time-continuous half-periodic signals to form signals with completed periods, which are defined as positive and negative components, collectively referred to as split components.
Step 6: Perform the FFT on the split components to obtain the $f_c$ and $f_o$ of the split components and evaluate the differences between the obtained frequency characteristics.
Step 7: Calculate the defined damage index according to Eq. (8) and all the frequency values obtained from the spectra in Step 6.

## 3. Numerical verifications

### 3.1. Cantilever beam with a breathing crack

A uniform concrete cantilever beam with a transverse through-width breathing crack is designed. The geometric parameters of this cantilever beam, including the length ($L$), width ($w$), height ($h$) and the material parameters, including elastic modulus ($E$), Poisson's ratio ($\nu$), density ($\rho$), are given in Tab. 1. The breathing crack is specified by two parameters, namely the relative location ratio, $\beta = l_c/L$, and the relative depth ratio, $\alpha = a/h$ where $a$ and $l_c$ are the crack depth and crack location away from the free end, respectively. The three-dimensional cantilever beam is established and discretized with eight-node solid elements using the finite element software ANSYS, as shown in Fig. 3.

In this study, the opening or closing behavior of the breathing crack is computed as a local contact problem in which the adjacent crack surfaces are identified as the contact-target surface pairs. With one crack surface as the target surface and the other as the contact surface, the contact behavior of a crack is studied using the surface-to-surface contact approach, as illustrated in Fig. 3. In this study, the augmented Lagrange algorithm embedded in ANSYS software without considering friction is chosen for the contact pair model. The parameters of the contact pair model are set as follow: normal penalty stiffness factor – 1.0, penetration tolerance factor – 0.1, contact detection on Gauss points.

### 3.2. Damage identification using DISTINCT method

To illustrate the procedure of damage identification using the DISTINCT method, the numerical results of an intact beam, designated “case d0″, and a breathing-crack beam, designated ”case d3″, with a relative location ratio of 3/5 and a relative depth ratio of 3/

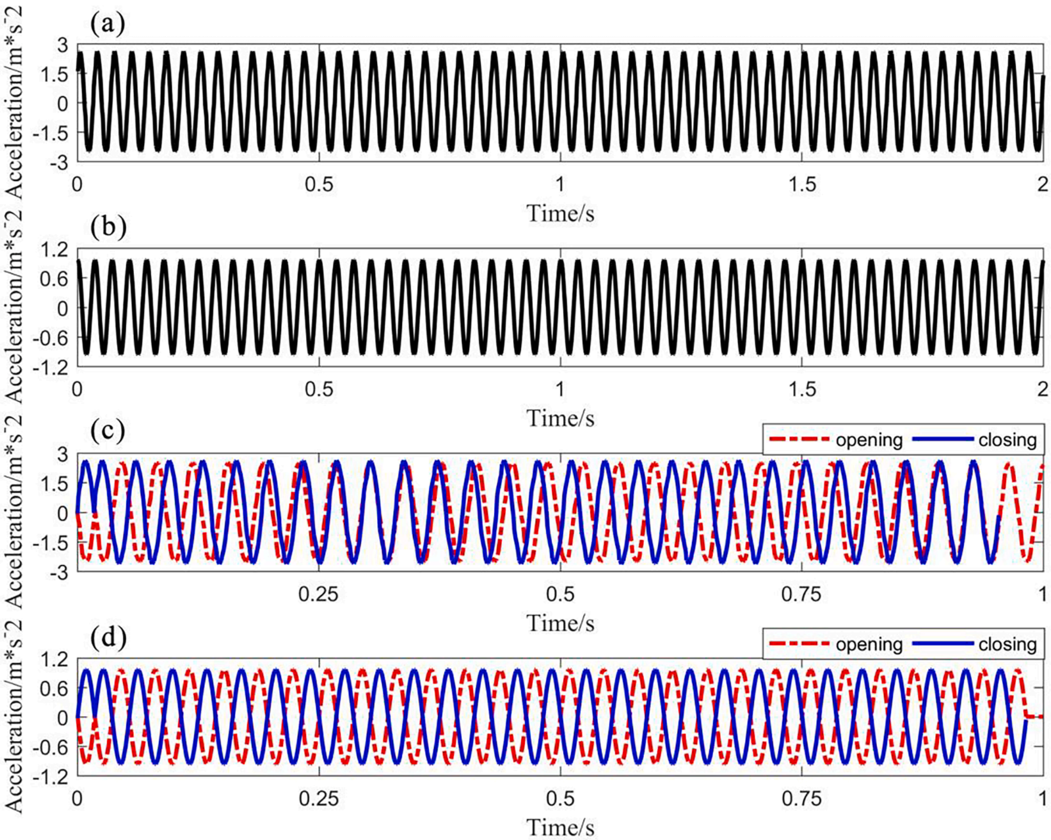


**Fig. 4.** Temporal responses, (a) original signal of “case d3″; (b) original signal of ”case d0″; (c) split components of “case d3″; (d) split components of ”case d0″.

6, are presented. The “case d3″ is arbitrarily selected as a representation of the damaged cases because the damage features that the method depends on can be typically found in both the time and frequency domains. Therefore, it should be pointed that the method is not only applicable in this particular case. A harmonic excitation with the intact beam fundamental frequency of 14 Hz is applied at two nodes on the upper surface of the beam free-end, as shown in Fig. 3. The amplitude and time duration of this harmonic excitation are 200 N and 10 s, respectively. The acceleration response along the beam length direction of the node 0.75 m away from the fixed end is collected. The numerical calculation of each damage case lasted for 10 s, the time step was 0.002 s, and the algorithm adopted the Newmark time integration method.

Fig. 4 displays the collected acceleration responses for “case d0″ and ”case d3″. The amplitude difference between the responses in the two cases is straightforward to be observed, but the difference in frequency between the two is not easy to detect due to the global vibration period is basically the same. The split components for both cases are obtained by performing steps 2–5 of the DISTINCT method on the original signals of “case d0″ and ”case d3″, respectively. In Fig. 4(c), the positive and negative components of “case d3″ are not synchronized in time. The duration of blue signal corresponding to the closing frequency is shorter than the duration of red signal corresponding to the opening frequency. However, as seen in Fig. 4(d), the red and blue lines derived via the DISTINCT of ”case d0″ are synchronized in time. This event indicates that the intact beam’s positive and negative components have the same frequency. Consequently, the frequency difference between the positive and negative components of the breathing-crack beam is expected be used to quantitatively assess the severity of breathing crack.

Fig. 5 shows the frequency distribution characteristics of the original response and the corresponding positive and negative components of “case d3″. The original signal has a main peak at around 14 Hz, representing the vibration characteristics of the cantilever beam in the breathing state, which is dominated by the excitation frequency. On either side of the main peak, at frequencies of 14.44 Hz and 13.63 Hz, respectively, are the peaks of the closing signal and the opening signal. This separation phenomenon indicates the existence of a breathing crack. In addition, there are still many super-harmonic components caused by breathing cracks in the high-frequency part (above the excitation frequency) of the original signal and the split components. However, the super-harmonic components of the split components present in pairs have different frequency characteristics from those of the original signal. As shown in Fig. 5, the distribution patterns of the original signal of ”case d3″ and the super-harmonic components of the split components are compared. The super-harmonic frequencies of the split components appear at odd multiples of the fundamental frequency, and their separation gradually increases with increasing multiples, from 43.33 and 40.89 Hz at 3 multiples to 245.1 and 231.3 Hz at 17 multiples. Nevertheless, the amplitude of the super-harmonic frequencies of the original signal at even multiples are much larger than that of the super-harmonic components at odd multiples.

The frequencies of all the peaks in Fig. 5 are extracted and integrated into Tab. 2 and Tab. 3. The closing frequency and its super-harmonic components are denoted by $f_c$. The opening frequency and its super-harmonic components are denoted by $f_o$. The original signal’s frequency and its super-harmonic components are denoted by $f_b$. The multiplicity, $n$, of super-harmonics are denoted by $nf$. $f_b^*$, the same as the original signal’s peak at odd multiples, is calculated directly from the closing and opening frequencies by Eq. (6), which proves that the numerical breathing-crack cantilever beam conforms to the assumption of a bilinear system. On the other hand, the separation degree of the super-harmonic components appearing in pairs of the split components is equal to the product of the separation degree of the fundamental frequency and the multiplicity of super-harmonics, regardless of its increase with the multiplicity of super-harmonics. As a result, the *DI* values of the fundamental frequency and its super-harmonic components calculated by Eq. (8) are also approximately equal. This feature suggests that the existence and assess the severity of breathing crack can be determined using the separation phenomena at both fundamental frequency and its odd multiples of super-harmonic components.

The frequency distribution characteristics of the original signal from “case d0″ are shown in Fig. 6, together with corresponding positive and negative components in the frequency domain. The original signal presents a main peak with a frequency of 14 Hz in the

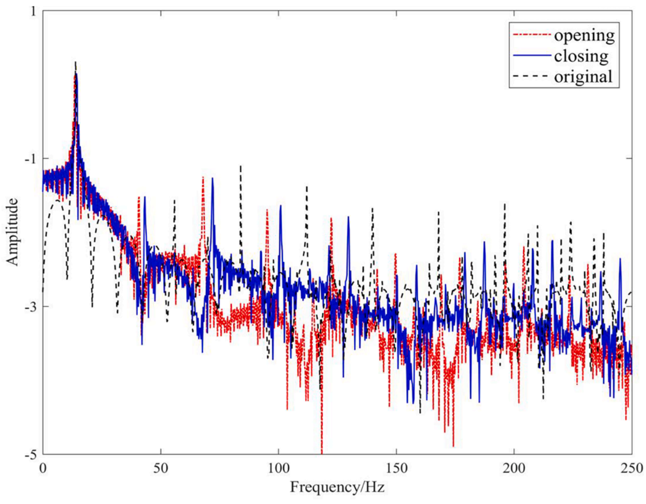


**Fig. 5.** Logarithmic frequency spectra of original signal and split components of “case d3″.

frequency domain, which is dominated by the applied excitation frequency. The fundamental frequency, where the original signal peaked, is where the opening and closing frequencies peaked. This phenomenon indicates that the frequency characteristics of the two split components, which are extracted from the original signal of the intact structure, are the same. Neither the two split components nor the original signal has super-harmonic components at the high-frequency part (above the excitation frequency) due to the structural integrity.

Similarly, several other numerical cantilever beams with the same relative position ratio – 3/5 and different relative depth ratios are used to investigate the effect of different crack depths. These numerical cantilever beams with relative depth ratios of 2/6, 3/6, 4/6, and 5/6 are designated as "case d2″, "case d3″, "case d4″ and "case d5″, respectively. These cases are executed with the same excitation conditions as above and the acceleration responses are collected. The split components corresponding to the acceleration responses are obtained after the execution of the DISTINCT method. Fig. 7 displays the split components' logarithmic frequency spectra. The separation degree of the split components increases with the crack depth at this position.

### 3.3. Characteristics of method

#### 3.3.1. Initial nonlinearity tolerance

The key superiority of this method is that the immune to the inherent nonlinearity. To verify this superiority, the input harmonic excitation is assumed to contain nonlinear components. The excitation is composed of simple harmonic components with frequencies at 14 Hz, 2 × 14 Hz, 3 × 14 Hz, 4 × 14 Hz, 5 × 14 Hz, and amplitude ratio at 4:1:1:1:1, respectively. The amplitude of the synthesized signal is set at 200 N, as shown in Fig. 8 (a). This nonlinear excitation is input to the two cases: "case d0″ and "case d3″ specified in section 3.2. Then, the responses of the "case d0″ and "case d3″ excited by the nonlinear excitation are shown in Fig. 8 (b) and Fig. 8 (c), respectively. The split components of "case d0″ and "case d3," which represent in an intact and cracked beam, respectively, are subjected to the FFT, and the corresponding results in the frequency domain are presented in Figs. 9 and 10.

Five harmonic components appear in the frequency domain of the original signal for the intact beam in Fig. 9. The frequency domain of the split components for the cracked beam, on the other hand, exhibits three harmonic components with frequencies of 14 Hz, 42 Hz, and 70 Hz. However, the three harmonic components are not separated, indicating that the beam does not have a breathing crack.

As shown in Fig. 10, for the beam with a breathing crack, there are many high-order harmonic components in the original signal, which is caused by both the input and the existence of the breathing crack. The peaks appear in the split component at odd times of the excitation frequency and the separation phenomenon exists. The frequencies of the peaks in Fig. 10 exactly match those shown in Fig. 5, although the input excitation is different.

In a word, when the excitation used to detect structural damage has nonlinear components or the excitation is not closely connected to the structure, the traditional method to measure the existence of breathing crack with the occurrence of higher harmonics will be misguided. However, the separation features used in the proposed method to measure breathing crack still work well.

#### 3.3.2. Frequency of excitation

The aforementioned analyses are conducted at the fundamental natural frequency of the numerical cantilever beam, but the fundamental natural frequency is generally not available in practice. Therefore, it is necessary to study how well the DISTINCT method works for non-fundamental frequency excitations.

Primarily, "case d3″ is excited with harmonic excitation below the fundamental frequency of the cantilever beam, including the harmonic excitations with frequency between 8 and 13 Hz. Fig. 11(a) shows the logarithmic frequency spectrum of the original signal

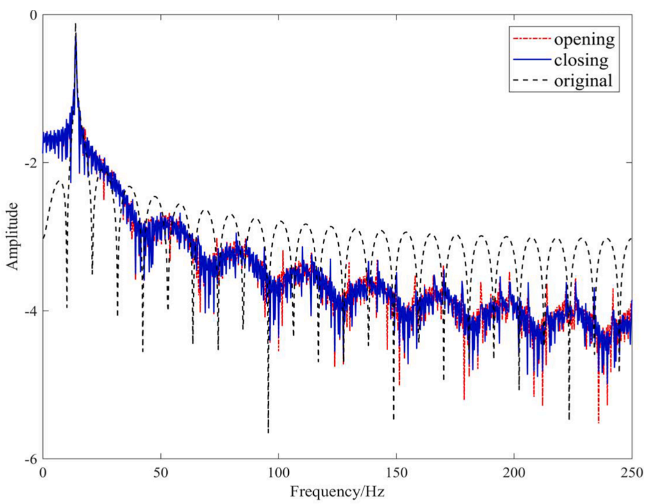


**Fig. 6.** Logarithmic frequency spectra of the original signal and split components of "case d0″.

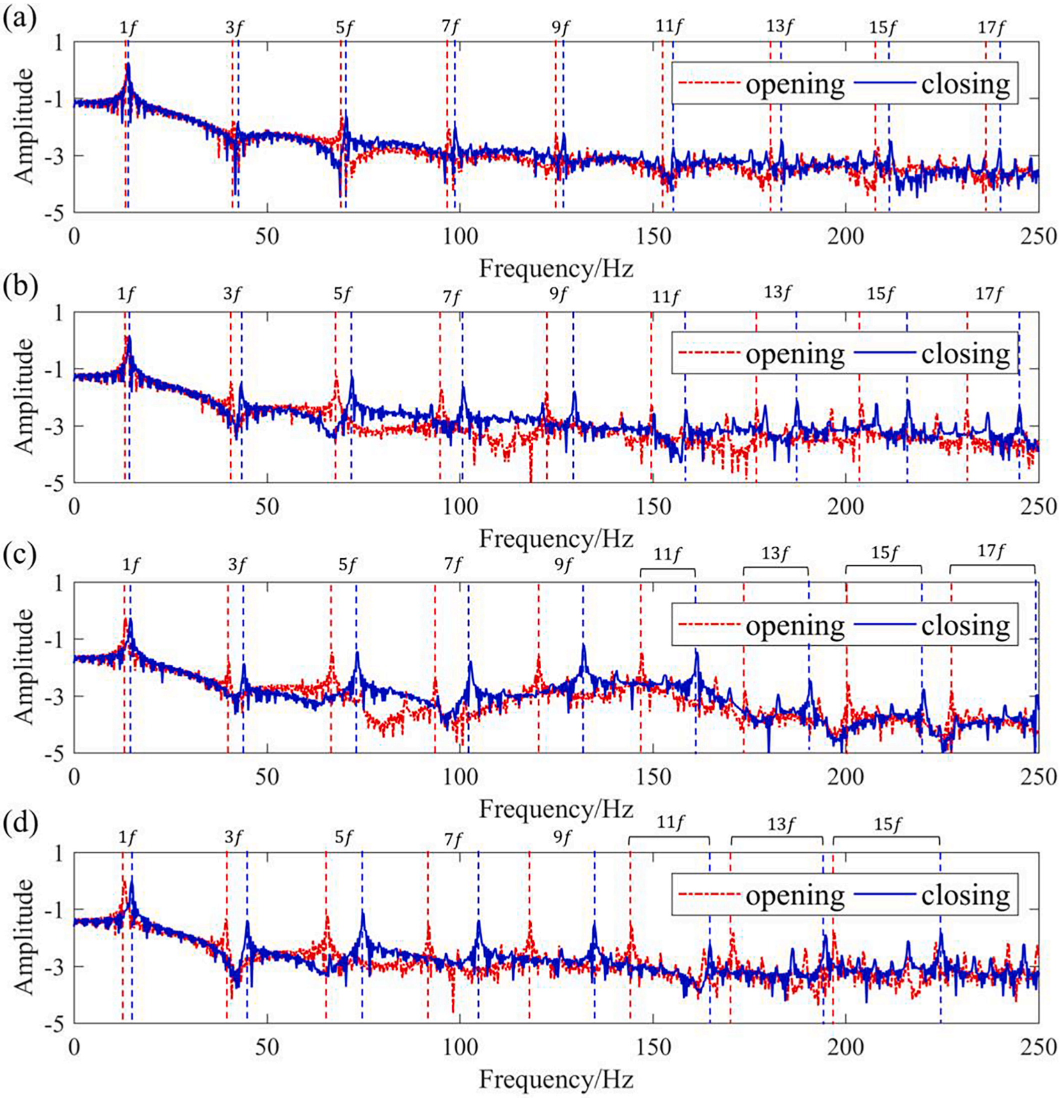


**Fig. 7.** Logarithmic frequency spectra of the split components, (a) “case d2″; (b) ”case d3″; (c) “case d4″; (d) ”case d5″.

and the two split components of the breathing-crack beam excited by 10 Hz harmonic excitation. It is observed that the opening and closing frequencies are located at both sides of 10 Hz, while their super-harmonic components appear at both sides at odd multiples of 10 Hz. The super-harmonic components of the original signal are mainly evident at even multiples of 10 Hz, and the intensity is very low at odd multiples of 10 Hz. The super-harmonic components of the original signal are mainly evident at even multiples of 10 Hz, but the intensity is very low at odd multiples of 10 Hz. The separation degree of the split components is different under these harmonic excitations which are below the fundamental frequency, even though the separation characteristics are the same.

Subsequently, the harmonic excitations with frequency at 15–50 Hz are applied to investigate the effectiveness of excitation frequencies above the fundamental frequency of the cantilever beam on the DISTINCT method. Fig. 11(b) shows the logarithmic frequency spectrum of the original signal and the two split components of the breathing-cracked beam excited by 30 Hz harmonic excitation. The separation characteristics of the split components excited by 15–34 Hz harmonic excitations are consistent with those driven by fundamental natural frequency excitation, but the separation degree varies with the excitation frequency. Fig. 11(c) shows the logarithmic frequency spectrum of the original signal and the two split components of the breathing-cracked beam excited by 37 Hz harmonic excitation. The amplitude at 2 multiples of the excitation frequency is higher than the amplitude at the excitation frequency. Thus, the split components are separated at 2 multiples of the excitation frequency. The separation of the split components in the high part (above 2 multiples of the excitation frequency) occurs at even multiples of the excitation frequency, rather than that at odd multiples of the excitation frequency. When the excitation is located in the 35–42 Hz interval, the separation phenomenon of the split components starts at 2 multiples of the excitation frequency and increases by 2 multiples of the excitation frequency. Fig. 11(d) shows the logarithmic frequency spectrum of the original signal and the two split components of the breathing-cracked beam excited by 45 Hz

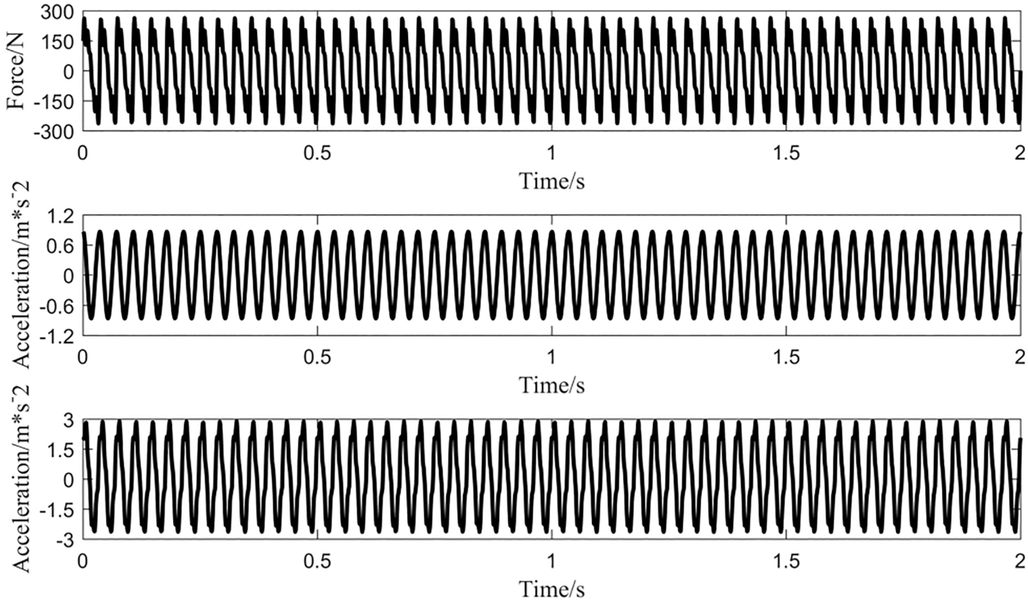


**Fig. 8.** Nonlinear excitation and acceleration responses, (a) excitation; (b) responses of "case d0″; (c) responses of "case d3″.

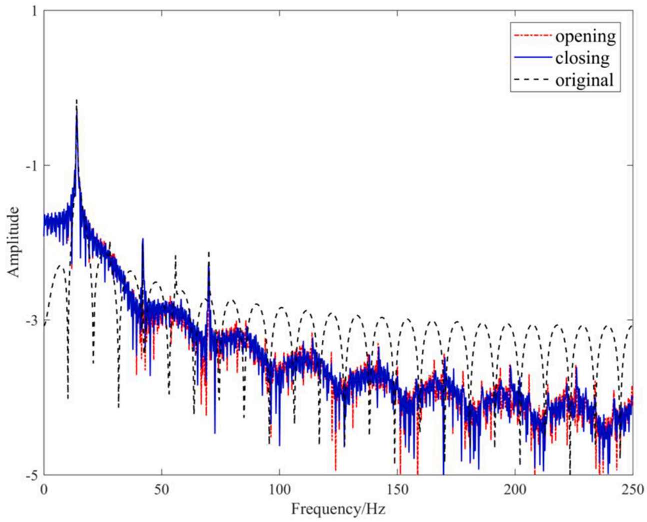


**Fig. 9.** Logarithmic frequency spectra of the split components of "case d0″.

harmonic excitation. The amplitude of the excitation frequency is again higher than that of 2 multiples of the excitation frequency. As a result, the separation phenomenon starts at the excitation frequency and increases by 2 multiples of the excitation frequency.

The core feature of this method is that the opening and closing frequencies/the multiples of opening and closing frequencies are distributed on both sides of the breathing frequency/the multiples of breathing frequency. The core feature is applicable to different excitation frequencies based on the above analysis. However, the final *DI* values obtained from the detected structure evoked by excitations with different frequencies are not the same. Therefore, the selection of multiple excitation frequencies is necessary for a comprehensive detection of the damage. The evaluation of the damage degree for different periods of the same structure requires the application of harmonic excitation with the same frequency.

### *3.3.3. Noise influence*

In practical scenarios of measuring dynamic responses with sensors, the noise components caused by various environmental sources, such as thermal noise, mechanical relaxation, and electrical noise in the data acquisition systems, are inevitably involved in the responses. In the assessment of any damage identification method, an effective identification of damage under noisy conditions is essential. To fulfil this requirement, the noise resistance of the proposed method is discussed. The Gaussian white noise is used in the

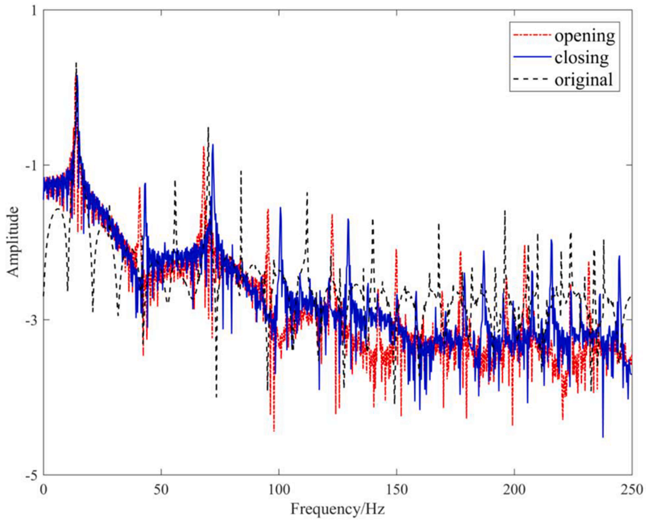


**Fig. 10.** Logarithmic frequency spectra of the split components of "case d3″.

structural damage identification and a signal noise ratio (SNR) definition is presented to label the noise level.

$$SNR = 20\log_{10}\left(\frac{A_{signal}}{A_{noise}}\right) \tag{9}$$

where, $A_{signal}$ and $A_{noise}$ denote the root mean square magnitude of the vibration signal and added noise, respectively.

The original time domain response of "case d3″ is added to various levels of noise and then subjected to the DISTINCT method. This response is forced by the fundamental frequency excitation, i.e., 14 Hz harmonic excitation. Fig. 12 displays the split components' logarithmic frequency spectra with varying levels of noise. The frequency seperation feature of the split components is very clearly observable in the absence of noise, or when the SNR=∞, as seen in Fig. 12(a). The odd number of separation frequencies from 1 to 17 multiples in pairs can be easily observed on the frequency domain. When the SNR equals 40 dB, the separation feature in odd multiples of the excitation frequency of the DISTINCT method still performs well and has a high discrimination. When the signal SNR equals 30 dB, the separation feature is highly discernible below 200 Hz and difficult to distinguish above 200 Hz. When the SNR equals 20 dB, the separation phenomenon of the split components is observed below the 7 multiples of fundamental frequency. When the SNR equals 10 dB, the separation phenomenon of the split components is observed below the 5 multiples of fundamental frequency. The peaks at other frequencies are drowned by the noise. Even so, the separation phenomenon of the split components at the fundamental frequency is still significant. The closing and opening frequencies at the fundamental frequency are consistently maintained at 14.44 Hz and 13.63 Hz at various noise levels.

The original signals' logarithmic frequency spectra for "case d3″ is shown in Fig. 13 along with various noise levels. The traditional nonlinear detection methods focus on the distribution characteristics of the peaks at the integer multiples of the excitation frequency, i. e., the super-harmonics. The appearance of super-harmonics is regarded as the basic condition for determining presence of breathing cracks and the amplitude relationship of super-harmonics is employed to assess the degree of damage. As shown in Fig. 13(a-c), the super-harmonic components at the noise levels of 40 dB and 30 dB are not significantly different from the noise-free state in frequency and amplitude, even though some broadband noise appear due to SNR decrease. The noise reaches nearly half of the true amplitude when the SNR drops to 20 dB. As a result, although the frequencies of peaks are accurate, the amplitude of peaks are no longer accurate. The majority of multiples of the excitation frequency are drowned out by noise when the SNR drops to 10 dB, making it impossible to assess the structural damage condition using the super-harmonic distribution features. In a word, while the traditional super-harmonics-based detection methods can assess the extent of damage under SNR = 30 dB level and the presence of damage under SNR = 20 dB level, the frequency separation of the DISTINCT method is effective under SNR = 10 dB level or even less.

The peak at the excitation frequency with high energy and amplitude has a good noise immunity when considering the influence of noise, while the other peaks are readily contaminated by noise. The requirement of the traditional method is that all the multiple peaks of the excitation frequency are clearly observed. As soon as separation takes place at the excitation frequency, the breathing crack can be identified, giving the DISTINCT method considerable noise immunity.

### 3.4. Generality of method

The above studies are carried out based on cantilever beams with a breathing crack. To investigate the applicability of the DISTINCT method to other structures, numerical calculations are also performed for the three-sided fixed shell. The finite element model and geometry layout of the breathing-cracked shell is shown in Fig. 14. The material parameters of the shell are shown in Tab. 1. The shell is a quarter of a cylindrical shell with a radius of 2 m, a height of 2 m, and a thickness of 0.1 m. The depth of the crack is

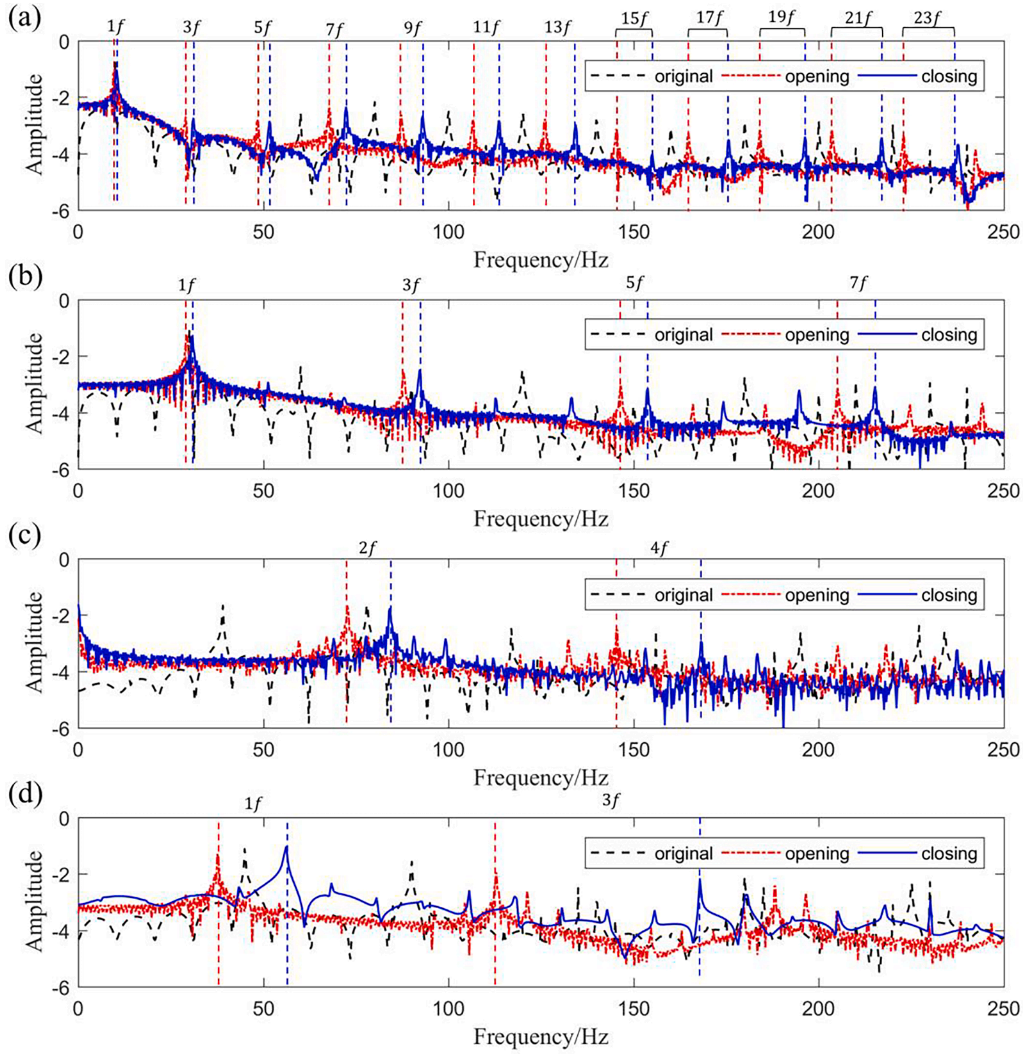


**Fig. 11.** Logarithmic frequency spectra of the original signal and split components for "case d3″ evoked by various harmonic excitations, (a) 10 Hz; (b) 30 Hz; (c) 37 Hz; (d) 45 Hz.

assumed to be 0.5 m. The finite element model of this shell is discretized through 1998 eight-node solid elements and 2944 nodes. The breathing crack simulated by using the contact model is assumed to be located at the top right side of the shell, and the remaining three sides are fixed. Similar to the crack simulation of the cantilever beam in Section 3.1, the crack here is also adopted as the contact pair model without considering friction. The parameters of the contact pair model are set as follow: normal penalty stiffness factor – 1.0, penetration tolerance factor – 0.1, contact detection on Gauss points. The acceleration responses perpendicular to the excitation direction (x-direction) are collected after applying a harmonic excitation along the normal direction of the shell with frequency at 100 Hz, which is below the fundamental frequency of the shell. The amplitude of this harmonic excitation is 200 N with duration at 10 s. The acceleration responses are collected for six nodes, labeled as a1–a6.

Fig. 15 displays the logarithmic frequency spectra of the original response and the split components of the breathing-cracked shell, respectively. As shown in Fig. 15 (a), (b), (d) and (e), the separations of the opening and closing frequencies for 'a1′', 'a2′', 'a4′' and 'a5′' are apparent at the excitation frequency, i.e., 100 Hz, and even at multiples of the excitation frequency, i.e., 200 Hz, 400 Hz, 600 Hz and 800 Hz. The separation features of the split components caused by the breathing crack satisfy the following: (i) the opening and closing frequencies conform to bilinear characteristics as described in Eq. (6); (ii) the separation interval of the opening and closing frequencies at multiples is equal to the product of the separation interval at the fundamental frequency and the multiples. As shown in Fig. 15 (c) and (f), the opening and closing frequencies coincide exactly with the original signal at the excitation frequency and odd multiples of the excitation frequency. The above analysis shows that the DISTINCT method is effective for detecting breathing crack in shell structure. However, the positioning of the sensor in this three-sided fixed-shell construction affects the extraction of damage features. The separation features can be captured more effectively by the sensors positioned on the crack's side.

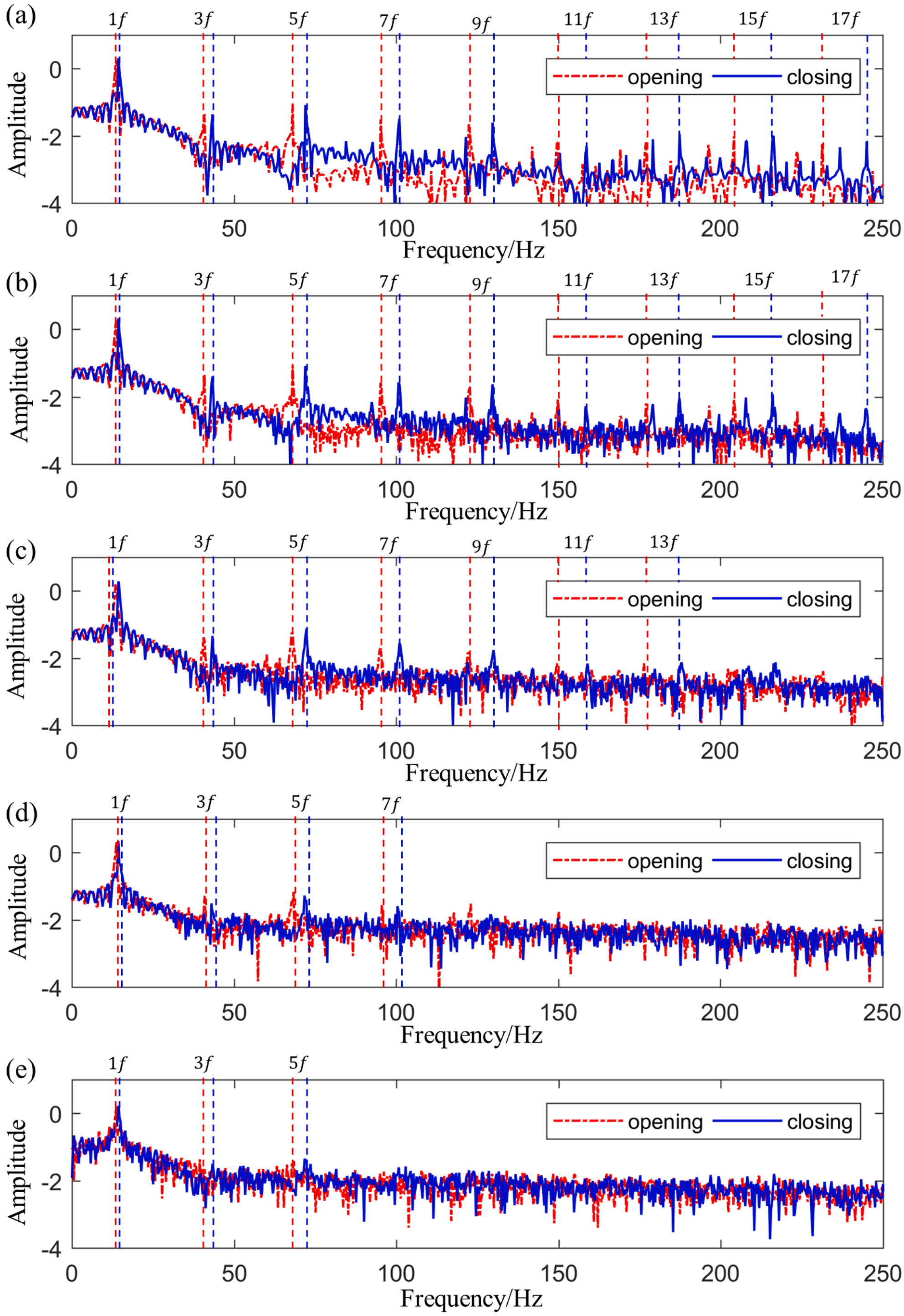


**Fig. 12.** Logarithmic frequency spectra of split components for "case d3" under noise conditions, (a) SNR=∞; (b) SNR = 40 dB; (c) SNR = 30 dB; (d) SNR = 20 dB; (e) SNR = 10 dB.

## 4. Experimental validation

### *4.1. Experiment description*

The transverse joints formed by grout sealing after the completion of each dam section are considered to be weak areas of the

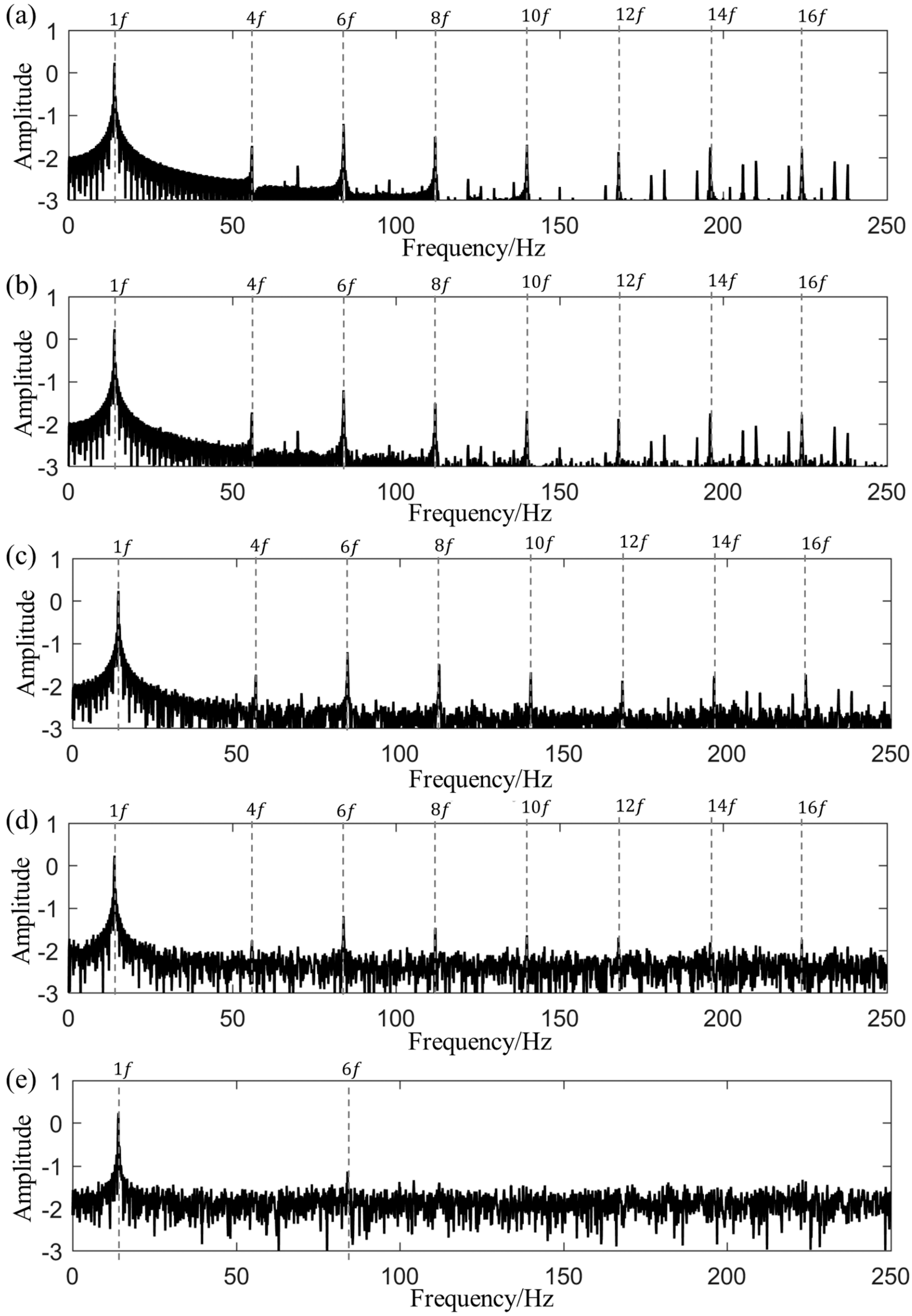


**Fig. 13.** Logarithmic frequency spectra of original signal for "case d3″ under noise conditions, (a) SNR=∞; (b) SNR = 40 dB; (c) SNR = 30 dB; (d) SNR = 20 dB; (e) SNR = 10 dB.

concrete arch dam structure and are susceptible to characteristics similar to breathing cracks under seismic dynamic action. A concrete arch dam with the height of 270 m located in southwest China is considered as the test prototype. The number of transverse joints is simplified to three. The scaled arch dam model with a geometric scale of 1:200 is manufactured and displayed in Fig. 16. Based on the similarity theory, a special material consisting of barite sand, barite powder, fly ash, cement and water, in the mass ratios of 5.28, 2.64, 0.6, 0.13 and 1, is designed to manufacture the scaled arch dam model. This model material has mechanical properties that are similar

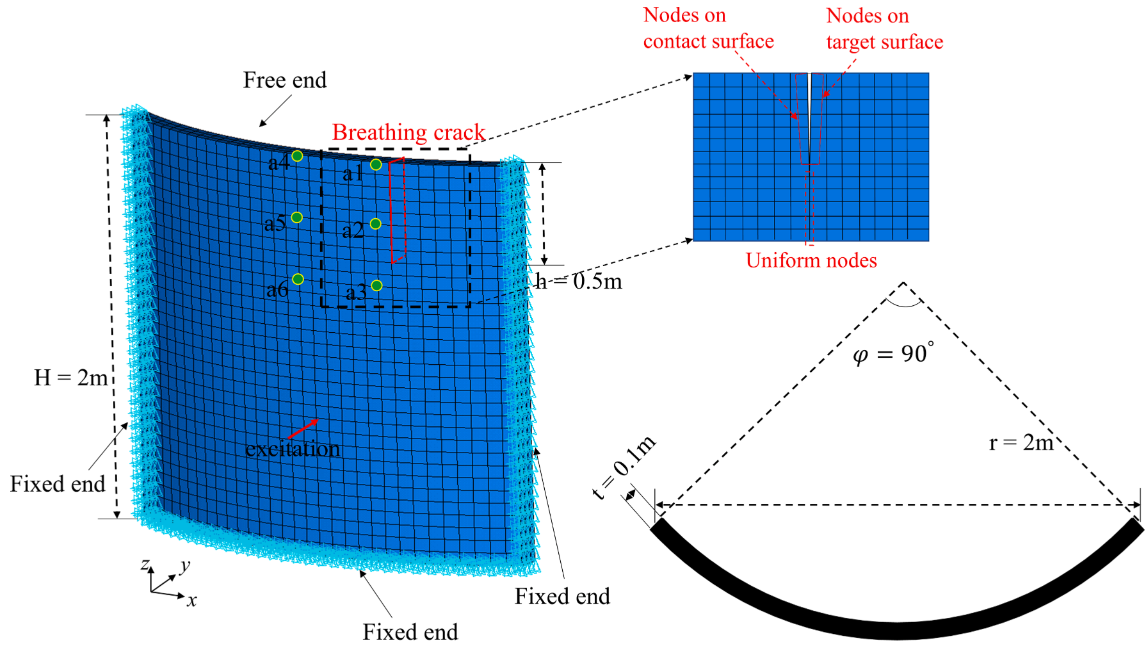


**Fig. 14.** Finite element model and size layout of a breathing-cracked shell.

to those of real concrete, i.e., regarding the required elasticity, brittleness, and density. The foundation of the arch dam model is made by casting with ordinary concrete, labeled C30.

As shown in Fig. 16, three transverse joints are predetermined for this arch dam model, which are considered to be the locations where damage may occur. The three transverse joints are manufactured by the following process: three open cracks are sawed at the corresponding positions using wire saws; the middle joints are grouted with high-strength (model material) material; and the two side joints are grouted with low-strength (1/3 the strength of the model material) material.

The seismic experiment of the scaled arch dam model is conducted on a shaking table with three directions and six degrees of freedom in Hohai University, China. The design of the working conditions and the loading sequence of this experiment are shown in Fig. 17. A harmonic load with a frequency of 30 Hz, duration of 20 s and amplitude of 0.1 g is applied before the destructive test to detect the initial nonlinearity of the model and shaking table system. Then artificial seismic accelerations with four peak acceleration levels of 0.2 g, 0.4 g, 0.8 g, and 1.6 g are successively applied to damage the transverse joints of the arch dam model. After each artificial load, a harmonic load with a frequency of 30 Hz, a duration of 10 s and an amplitude of 0.2 g is applied to detect the damage caused by that level of artificial load. The direction of excitation is along the river, and the direction of acceleration sensor is perpendicular to the dam face. The responses of the arch dam model under seismic and harmonic loads are measured by accelerometers, labeled DH1A731E, with a sensitivity coefficient of 10 mV/g and measuring range of 50 g. These accelerometers are attached to the upstream surface of the dam model, and their positions are displayed in Fig. 16. The sampling frequency of the acquisition system is set at 2000 Hz. This study mainly focuses on the responses collected by the accelerometer labeled with the ellipse in Fig. 16.

During each simple harmonic excitation, optical measurements are carried out simultaneously on the downstream face of the dam to assist in the acquisition of the dam's behavior. The optical measurement method is based on high-speed cameras and digital image correlation techniques. The final strain diagram of the dam model in the X-direction subject to the harmonic excitation is shown in Fig. 18. There is significant damage at the transverse joint near the right bank, indicating that the transverse joint is pulled apart by the seismic acceleration, while the damage at the transverse joint near the left bank is not significant.

### *4.2. Accommodation of inherent nonlinearity*

Prior to the destructive testing, the initial structural characteristics are assessed using harmonic excitation in order to identify the inherent nonlinearity of the scaled arch dam model and the shaking table system as well as to verify the immunity of the DISTINCT approach to the inherent nonlinearity. The acceleration responses of the dam body are collected, and the split components of the original response are obtained according to steps 2–5 of the DISTINCT method. The corresponding logarithmic frequency spectra obtained by executing the FFT on the original signal and the split components are displayed in logarithmic form. As shown in Fig. 19 (a), the original signal has a main peak at 30 Hz, which corresponds to the frequency of the harmonic excitation. In the higher frequency part of the spectrum, many super-harmonic components, such as at frequencies of 60 Hz, 90 Hz, 120 Hz, 150 Hz and 180 Hz, are also found with some peaks. The presence of these super-harmonics implies the existence of cracks in the scaled arch dam model if the traditional super-harmonics-based nonlinear damage detection method is followed. However, the scaled arch dam model in this state is not damaged. Therefore, the presence of these super-harmonics indicates that the system of the scaled arch dam model and

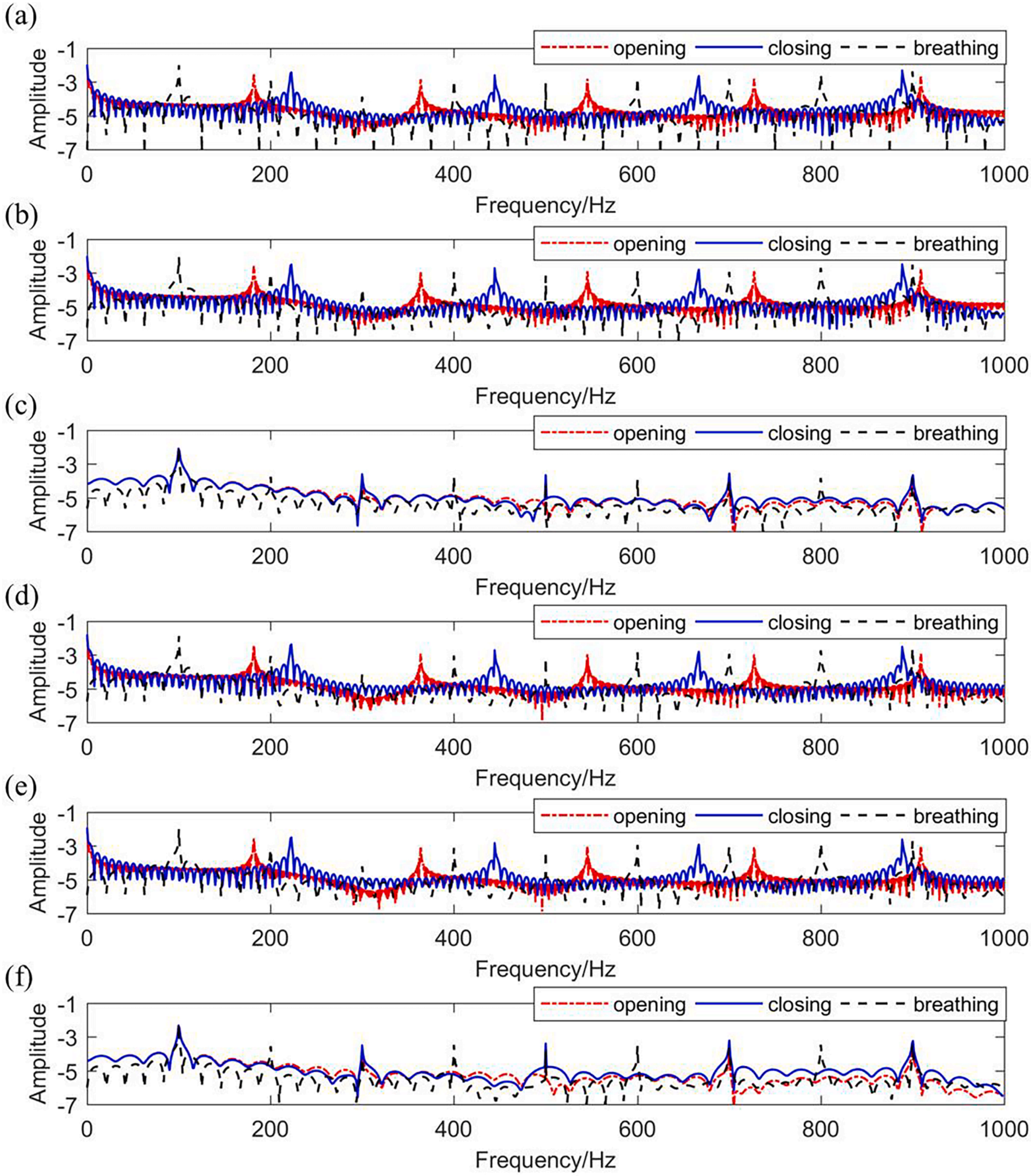


**Fig. 15.** Logarithmic frequency spectra of the original signal and the split components of the breathing-cracked shell at different positions, (a) position: a1; (b) position: a2; (c) position: a3; (d) position: a4; (e) position: a5; (f) position: a6.

shaking table is inherently nonlinear even when the arch dam model is intact. This inherent nonlinearity can be thought to be caused by the connection between the model and the shaking table, or it can be thought to be caused by the mechanics inside the shaking table. As shown in Fig. 19(b), the split components also have main peaks at 30 Hz, and both the opening and closing frequencies are simultaneously located at 30 Hz. Due to the presence of the inherent nonlinearity in the scaled arch dam model and shaking table system, the split components also show peaks at odd multiples of 30 Hz, i.e., 90 Hz, 150 Hz, and 210 Hz. However, the opening and closing frequencies are not separated, which indicates that the inherent nonlinearity has the same effect on the opening and closing frequencies. This un-separation of the split components in frequency is completely different from the opening and closing frequency

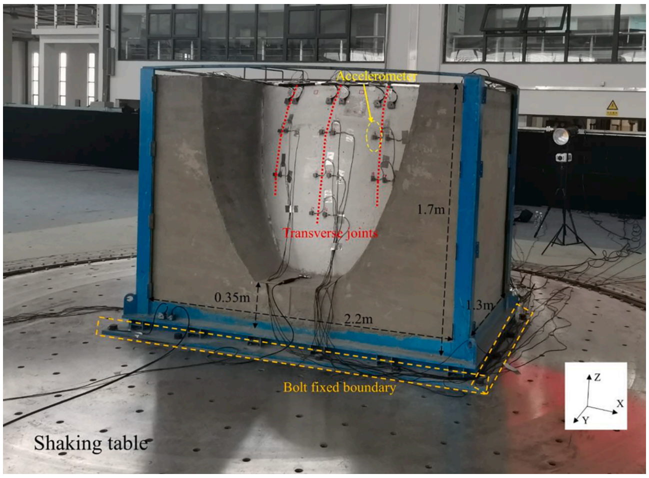


**Fig. 16.** Scaled model of the arch dam on a shaking table.

| Name | Load direction | | Duration (s) | Frequency (Hz) | Amplitude (g) |
|---|---|---|---|---|---|
| | X | Y | | | |
| Test1 | | 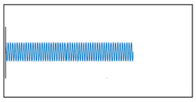 | 20 | 30 | 0.1 |
| Test2 | 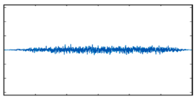 | 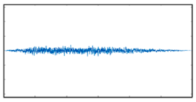 | 60 | 0–200 | 0.2 |
| Test3 | | 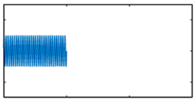 | 10 | 30 | 0.2 |
| Test4 | 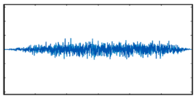 | 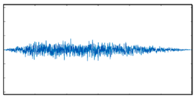 | 60 | 0–200 | 0.4 |
| Test5 | | 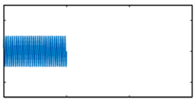 | 10 | 30 | 0.2 |
| Test6 | 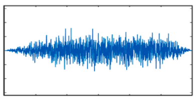 | 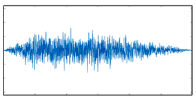 | 60 | 0–200 | 0.8 |
| Test7 | | 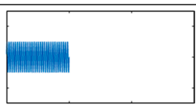 | 10 | 30 | 0.2 |
| Test8 | 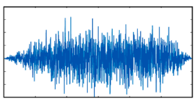 | 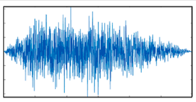 | 60 | 0–200 | 1.6 |
| Test9 | | 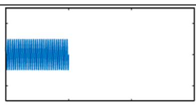 | 10 | 30 | 0.2 |

**Fig. 17.** Loading sequences and parameters setting.

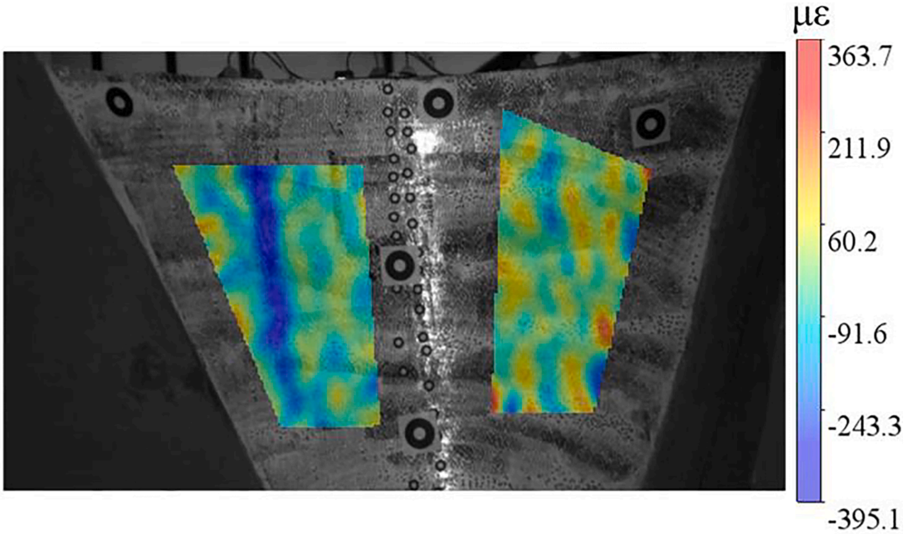


**Fig. 18.** Lagrange strain in the X direction captured by optical technology.

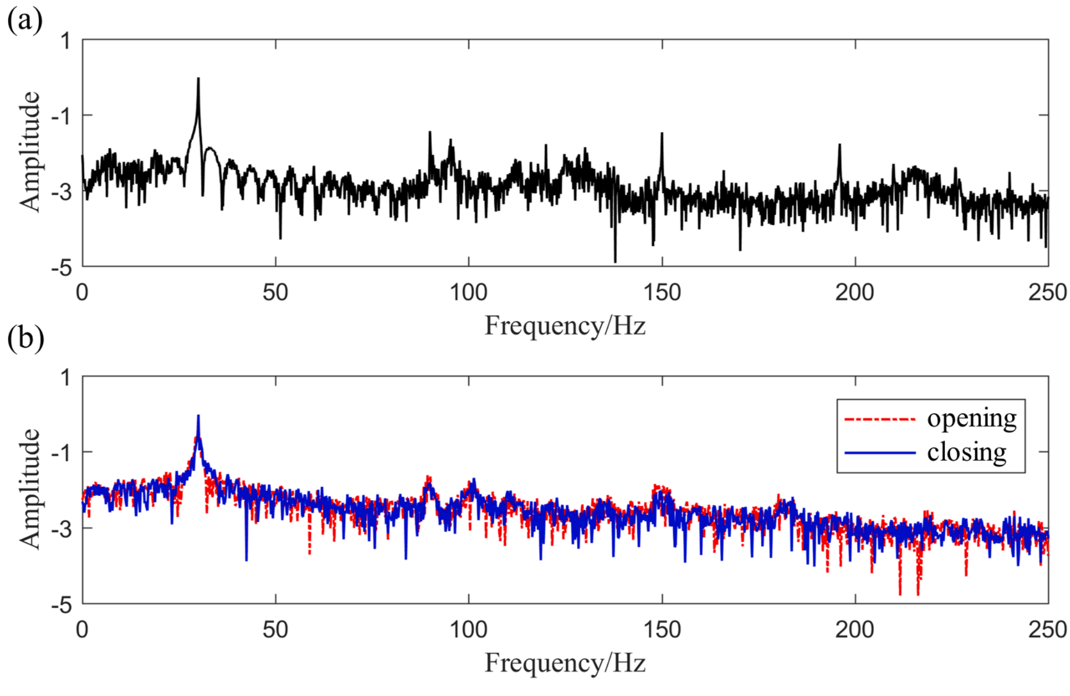


**Fig. 19.** Logarithmic frequency spectra for the scaled arch dam in the initial state, (a) original signal; (b) split components.

separation caused by breathing cracks. That is to say that the DISTINCT method has the ability to accommodate the inherent nonlinearity.

### 4.3. Damage identification using DISTINCT

Four levels of artificial loads caused four levels of damage to the scaled arch dam model, especially to the transverse joints, which are considered weak areas. A harmonic load in the direction along the river is applied to detect the damage after each artificial load. The acceleration responses in the loading direction are recorded by the accelerometer on the arch dam body during each detective harmonic load. The DISTINCT procedure is performed on the collected acceleration responses, and the frequency spectra of the original responses and split components are obtained by the FFT, as shown in Fig. 20.

Fig. 20(a) shows that the closing and opening frequencies of the scaled arch dam model no longer remain at 30 Hz (initial state) after the first-level of damage but change to 30.27 Hz and 29.79 Hz, respectively. This slight separation of the frequencies of the two split components of the original signal indicates that the transverse joints of the scaled arch dam model are slightly damaged. As shown in Fig. 20(b), there is an obvious separation between the closing and opening frequencies after the second-level damage. The two split frequencies of the excitation frequency are 30.52 Hz and 29.54 Hz, respectively. This obvious separation indicates that the scaled arch dam shows a breathing behavior induced by the damage in the transverse joints under the action of harmonic load. As shown in Fig. 20 (c) and (d), there is an increasing separation between the closing and opening frequencies after the third and fourth destructive seismic accelerations. The frequencies of the two split components after the third-level damage are 31.49 Hz and 28.56 Hz, and the frequencies of the two split components after the fourth-level damage are 32.47 Hz and 27.83 Hz. These phenomena indicate that the breathing behavior of the scaled arch dam becomes more apparent and the damage at the transverse joints becomes more severe with the increase of the destructive seismic acceleration intensity (Tables 1–3).

Table 4 presents the frequency values of the split components of the four harmonic vibration responses at the odd multiples of the excitation frequency. $f_c$ and $f_o$ represent the closing and opening frequencies, respectively; $f_b^*$ represents the breathing frequency calculated according to Eq. (6) based on the closing and opening frequencies, and $f_b$ represents the breathing frequency extracted directly from the spectrum of the original signal. The breathing frequencies of the original signal and the breathing frequencies calculated by the frequencies of the split components are basically equal, which proves that this scaled arch dam model also conforms well to the bilinear assumption with damage in the transverse joints. On the other hand, the *DI* values calculated from either the

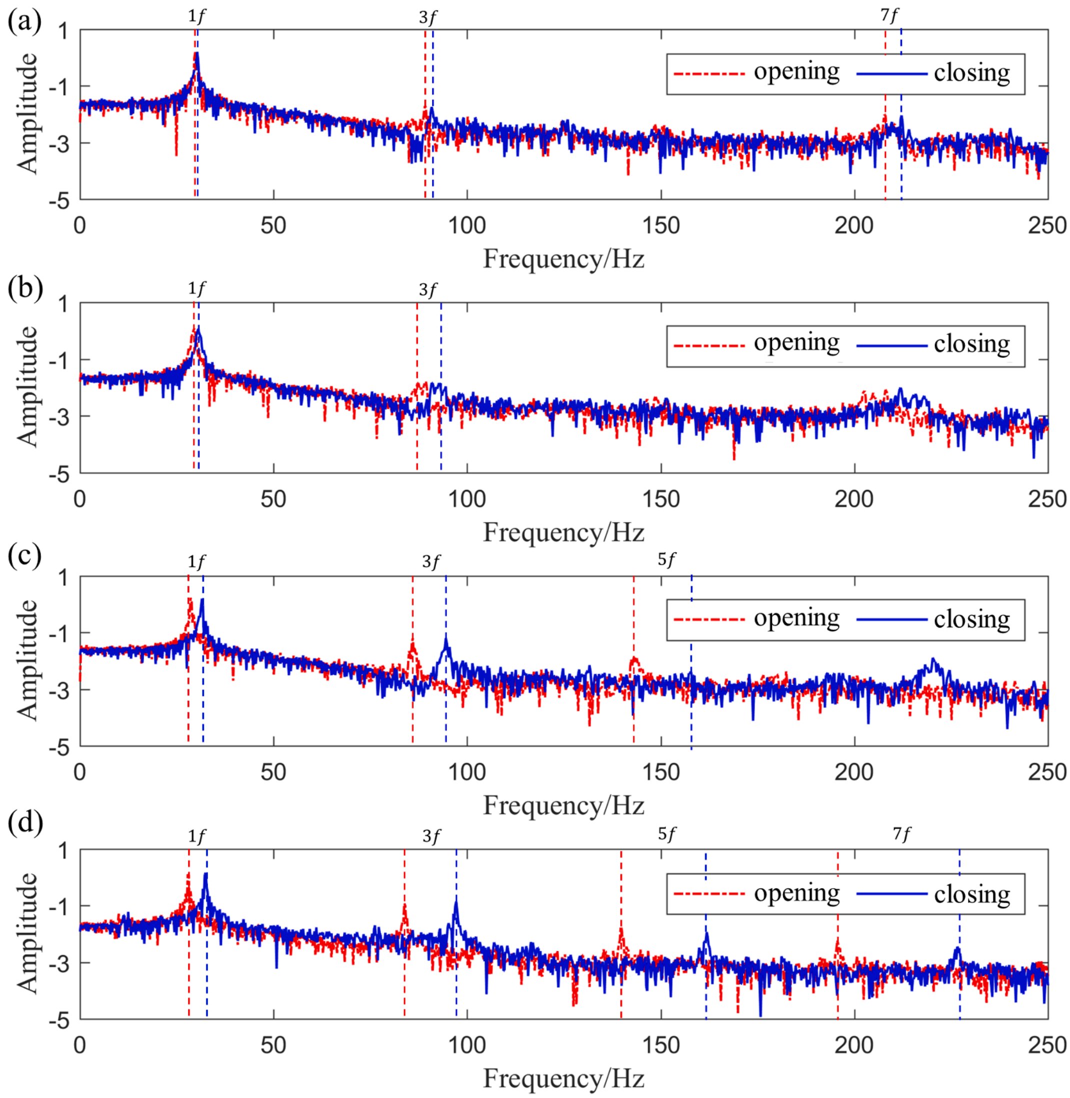


**Fig. 20.** Logarithmic frequency spectra of the split components of the scaled arch dam, (a) first-level damage; (b) second-level damage; (c) third-level damage; (d) fourth-level damage.

**Table 1**
Parameters of the breathing-crack cantilever beam model.

| Type | $L$ | $w$ | $h$ | $E$ | $\nu$ | $\rho$ |
|---|---|---|---|---|---|---|
| Unit | m | m | m | Pa | 1 | kg/m$^3$ |
| Value | 5 | 0.4 | 0.6 | $3 \times 10^{10}$ | 0.2 | 2400 |

**Table 2**
Identified multiple frequencies of split components.

| Multiple | 1 $f$ | 3 $f$ | 5 $f$ | 7 $f$ | 9 $f$ | 11 $f$ | 13 $f$ | 15 $f$ | 17 $f$ |
|---|---|---|---|---|---|---|---|---|---|
| $f_c$(Hz) | 14.44 | 43.33 | 72.02 | 101.00 | 129.70 | 158.70 | 187.40 | 216.40 | 245.10 |
| $f_o$(Hz) | 13.63 | 40.89 | 68.05 | 95.21 | 122.40 | 149.80 | 177.00 | 204.20 | 231.30 |
| $f_b^*$(Hz) | 14.02 | 42.07 | 69.98 | 98.02 | 125.94 | 154.12 | 182.05 | 210.12 | 238.00 |
| $DI$ (%) | 5.77 | 5.80 | 5.67 | 5.91 | 5.80 | 5.77 | 5.71 | 5.81 | 5.80 |

**Table 3**
Identified multiple frequencies of original signal.

| Odd multiple | 1 $f$ | 3 $f$ | 5 $f$ | 7 $f$ | 9 $f$ | 11 $f$ | 13 $f$ | 15 $f$ | - |
|---|---|---|---|---|---|---|---|---|---|
| $f_b$(Hz) | 14.04 | 41.99 | 69.95 | 98.04 | 126.00 | 153.95 | 182.00 | 210.05 | – |
| Even multiple | – | 2 $f$ | 4 $f$ | 6 $f$ | 8 $f$ | 10 $f$ | 12 $f$ | 14 $f$ | 16 $f$ |
| $f_b$(Hz) | – | 28.08 | 55.91 | 83.98 | 112.10 | 139.90 | 168.00 | 196.00 | 224.10 |

fundamental frequency separation or its odd-multiple separation are approximately equal at any level of damage, demonstrating the applicability of this super-harmonic separation feature for damage detection of the arch dam. These *DI* values obtained by the proposed DISTINCT method are located in the four intervals of 1.6–2.1%, 3.26–4.34%, 9.49–9.78%, and 14.76–15.48% for the four levels of damage condition, respectively. Innovatively, these *DI* values can better reflect the damage severity of the transverse joints.

## 5. Conclusions

A simple and effective method with inherent nonlinearity tolerated for assessing breathing cracks is developed based on nonlinear dynamic feature of breathing cracks. Both numerical verifications and experimental validations demonstrate the effectiveness and superiority of the proposed DISTINCT method to the traditional method. The main conclusions that can be drawn are as follows:

(1) In this method, the whole structural response in the breathing state is split into closing and opening components by zero-point search and techniques, such as signal splitting and flipping. The difference in frequency between the closing and opening components is the damage feature for detecting breathing cracks in the structure.

**Table 4**
Closing frequencies, opening frequencies and breathing frequencies of the scaled arch dam in four levels of damage.

| Damage severity | Type | 1 $f$ | 3 $f$ | 5 $f$ | 7 $f$ |
|---|---|---|---|---|---|
| I | $f_c$(Hz) | 30.27 | 90.82 | / | 212.20 |
| | $f_o$(Hz) | 29.79 | 89.11 | / | 207.80 |
| | $f_b^*$(Hz) | 30.03 | 89.96 | / | 209.98 |
| | $f_b$(Hz) | 30.03 | 90.09 | / | 210.00 |
| | $DI$ (%) | 1.60 | 1.90 | / | 2.10 |
| II | $f_c$(Hz) | 30.52 | 92.04 | / | / |
| | $f_o$(Hz) | 29.54 | 88.13 | / | / |
| | $f_b^*$(Hz) | 30.02 | 90.04 | / | / |
| | $f_b$(Hz) | 30.03 | 90.09 | / | / |
| | $DI$ (%) | 3.26 | 4.34 | / | / |
| III | $f_c$(Hz) | 31.49 | 94.48 | 157.70 | / |
| | $f_o$(Hz) | 28.56 | 85.94 | 143.30 | / |
| | $f_b^*$(Hz) | 29.95 | 90.01 | 150.16 | / |
| | $f_b$(Hz) | 30.03 | 90.09 | 150.00 | / |
| | $DI$ (%) | 9.78 | 9.49 | 9.59 | / |
| IV | $f_c$(Hz) | 32.47 | 97.17 | 161.90 | 226.60 |
| | $f_o$(Hz) | 27.83 | 83.74 | 139.60 | 195.60 |
| | $f_b^*$(Hz) | 29.97 | 89.96 | 149.93 | 209.96 |
| | $f_b$(Hz) | 30.03 | 89.97 | 150.00 | 209.80 |
| | $DI$ (%) | 15.48 | 14.93 | 14.87 | 14.76 |

(2) This method has applicability in different structures and satisfies two essential features: the separation phenomenon of opening frequency and closing frequency exists in the super-harmonic components; the relationship between opening frequency, closing frequency and breathing frequency satisfies the bilinear assumption.
(3) This method does not require the structure to get response under the excitation of fundamental natural frequency. The excitations of other frequencies are also compatible with DISTINCT method. There are differences in *DI* values under different excitation frequencies, so the damage detection for a structure at different periods must be carried out at the same excitation frequency.
(4) This method has proved to be of stronger noise resistance than the traditional method for detecting breathing cracks. This method will not be affected by the non-damage nonlinear factors which commonly impair the capability of traditional methods for portraying damage.

The clarification of optimal excitation frequency to identify damage extents in different structures and the adaptability of the proposed method for crack localization in structures are worthy of further exploration in depth.

## Declaration of Competing Interest

The authors declare that they have no known competing financial interests or personal relationships that could have appeared to influence the work reported in this paper.

## Data availability

The data that has been used is confidential.

## Acknowledgements

The authors are grateful for the support from the Postgraduate Research & Practice Innovation Program of Jiangsu Province (No. KYCX22_0589), the Nanjing International Joint Research and Development Program (No. 202112003), and the Jiangsu International Joint Research and Development Program (No. BZ2022010), the Fundamental Research Funds for the Central Universities (No. B220204002).

## References

[1] S.A. Berg, K. Podgórski, I. Rychlik, Fatigue damage assessment for a spectral model of non-Gaussian random loads, Probab. Eng. Mech. 24 (2009) 608–617.
[2] P. Cawley, Non-destructive testing—current capabilities and future directions, Proceed. Institut. Mechan. Eng., Part L: J. Mate. Desig. Appl. 215 (2001) 213–223.
[3] B.W. Drinkwater, P.D. Wilcox, Ultrasonic arrays for non-destructive evaluation: A review, NDT E Int. 39 (2006) 525–541.
[4] S. Das, P. Saha, S.K. Patro, Vibration-based damage detection techniques used for health monitoring of structures: a review, Journal of Civil, Struct. Health Monit. 6 (2016) 477–507.
[5] N. Tandon, A. Choudhury, A review of vibration and acoustic measurement methods for the detection of defects in rolling element bearings, Tribol. Int. 32 (2000) 469–480.
[6] D. Goyal, B.S. Pabla, The Vibration Monitoring Methods and Signal Processing Techniques for Structural Health Monitoring: A Review, Arch. Comput. Meth. Eng. 23 (2016) 585–594.
[7] F. MagalhaEs, A. Cunha, E. Caetano, Vibration based structural health monitoring of an arch bridge: From automated OMA to damage detection, Mech. Syst. Sig. Process. 28 (2012) 212–228.
[8] F. Garescì, L. Catalano, F. Petrone, Experimental Results of a Damage Detection Methodology using Variations in Modal Parameters, Exp. Mech. 46 (2006) 441–451.
[9] W.X. Ren, G.D. Roeck, Structural Damage Identification using Modal Data. I: Simulation Verification, J. Struct. Eng. 128 (2002) 87–95.
[10] G. Sha, M. Radzieński, M. Cao, W. Ostachowicz, A novel method for single and multiple damage detection in beams using relative natural frequency changes, Mech. Syst. Sig. Process. 132 (2019) 335–352.
[11] G. Kawiecki, Modal damping measurement for damage detection, Smart Mater. Struct. 10 (2001) 466.
[12] Z. Zhang, G. Hartwig, Relation of damping and fatigue damage of unidirectional fibre composites, Int. J. Fatigue 24 (2002) 713–718.
[13] J.T. Kim, Y.S. Ryu, H.M. Cho, N. Stubbs, Damage identification in beam-type structures: frequency-based method vs mode-shape-based method, Eng. Struct. 25 (2003) 57–67.
[14] C. Zang, M. Imregun, Combined neural network and reduced FRF techniques for slight damage detection using measured response data, Arch. Appl. Mech. 71 (2001) 525–536.
[15] J. Li, S.S. Law, Y. Ding, Substructure damage identification based on response reconstruction in frequency domain and model updating, Eng. Struct. 41 (2012) 270–284.
[16] Z. Duan, G. Yan, J. Ou, B.F. Spencer, Damage localization in ambient vibration by constructing proportional flexibility matrix, J. Sound Vib. 284 (2005) 455–466.
[17] M.M. Alamdari, J. Li, B. Samali, FRF-based damage localization method with noise suppression approach, J. Sound Vib. 333 (2014) 3305–3320.
[18] A. Bovsunovsky, C. Surace, Non-linearities in the vibrations of elastic structures with a closing crack: A state of the art review, Mech. Syst. Sig. Process. 62–63 (2015) 129–148.
[19] J. Prawin, Localization of Breathing Crack in Beam-Like Structures Using Superharmonic Components Based on Singular Value Decomposition Approach, Int. J. Struct. Stab. Dyn. 20 (2019) 2050014.
[20] X.Q. Zhu, H. Hao, Damage detection of RC slabs using nonlinear vibration features, Int. J. Struct. Stab. Dyn. 9 (2009) 687–709.
[21] O. Giannini, P. Casini, F. Vestroni, Nonlinear harmonic identification of breathing cracks in beams, Comput. Struct. 129 (2013) 166–177.
[22] L. Yang, M. Ma, S. Wu, X. Chen, R. Yan, Z. Mao, An improved analytical dynamic model for rotating blade crack: With application to crack detection indicator analysis, J. Low Frequ. Noise Vibrat. Active Cont. 40 (2021) 1935–1961.
[23] L. Yang, X. Chen, S. Wang, A novel amplitude-independent crack identification method for rotating shaft, Proceed. Institut. Mechan. Eng. Part C-J. Mechan. Eng. Sci., 232 (2018) 4098-4112.

[24] K.V. Nguyen, Comparison studies of open and breathing crack detections of a beam-like bridge subjected to a moving vehicle, Eng. Struct. 51 (2013) 306–314.
[25] B. Wimarshana, F. Goes, N. Wu, C. Wu, Experimental study on breathing crack detection and evaluation under random loading with entropy, Trans. Can. Soc. Mech. Eng. 41 (2017) 669–680.
[26] M. Carminati, S. Ricci, Structural Damage Detection Using Nonlinear Vibrations, Int. J. Aerospace Eng. 2018 (2018) 1–21.
[27] F.E. Dotti, V. Cortínez, F. Reguera, Non-Linear dynamic response to simple harmonic excitation of a thin-walled beam with a breathing crack, Appl. Math. Model. 40 (2015) 451–467.
[28] C. Courtney, S.A. Neild, P.D. Wilcox, B.W. Drinkwater, Application of the bispectrum for detection of small nonlinearities excited sinusoidally, J. Sound Vib. 329 (2010) 4279–4293.
[29] S.A. Neild, M.S. Williams, P.D. Mcfadden, Nonlinear Vibration Characteristics of Damaged Concrete Beams, J. Struct. Eng. 129 (2003) 260–268.
[30] L.H. Wang, X.Y. Zhou, L. He, W.M. Yan, Damage detection of RC beams based on experiment and analysis of nonlinear dynamic characteristics, Constr. Build. Mater. 29 (2012) 420–427.
[31] G. Chen, X. Yang, X. Ying, A. Nanni, Damage detection of concrete beams using nonlinear features of forced vibration, Struct. Health Monit. 5 (2006) 125–141.
[32] U. Andreaus, P. Baragatti, Experimental damage detection of cracked beams by using nonlinear characteristics of forced response, Mech. Syst. Sig. Process. 31 (2012) 382–404.
[33] Z. Lu, Y. Lv, H. Ouyang, A super-harmonic feature based updating method for crack identification in rotors using a kriging surrogate model, Appl. Sci. 9 (2019) 2428.
[34] L. Yang, Z. Mao, S. Wu, X. Chen, R. Yan, Nonlinear dynamic behavior of rotating blade with breathing crack, Frontiers of, Mech. Eng. 16 (2021) 196–220.
[35] X. Wang, D. Liu, J. Zhang, Y. Jiao, Damage identification for nonlinear fatigue crack of cantilever beam under harmonic excitation, Journal of Vibroengineering 24 (2022) 435–452.
[36] T. Al-Hababi, M. Cao, N.F. Alkayem, B. Shi, Q. Wei, L. Cui, D. Umarac, M. Ragulskis, The dual Fourier transform spectra (DFTS): a new nonlinear damage indicator for identification of breathing cracks in beam-like structures, Nonlinear Dyn. 110 (2022) 2611–2633.
[37] G. Yan, A. De Stefano, E. Matta, R. Feng, A novel approach to detecting breathing-fatigue cracks based on dynamic characteristics, J. Sound Vib. 332 (2013) 407–422.
[38] Y.H. Huang, J.E. Chen, W.M. Ge, X.L. Bian, W.H. Hu, Research on geometric features of phase diagram and crack identification of cantilever beam with breathing crack, Results Phys. 15 (2019), 102561.
[39] S. Voggu, S. Sasmal, Dynamic nonlinearities for identification of the breathing crack type damage in reinforced concrete bridges, Struct. Health Monit. 20 (2020) 339–359.
[40] U. Andreaus, P. Baragatti, Cracked beam identification by numerically analysing the nonlinear behaviour of the harmonically forced response, J. Sound Vib. 330 (2011) 721–742.
[41] L.G.G. Villani, D.S. Samuel, C. Americo, Damage detection in uncertain nonlinear systems based on stochastic Volterra series, Mech. Syst. Sig. Process. 125 (2019) 288–310.
[42] A. Chatterjee, Structural damage assessment in a cantilever beam with a breathing crack using higher order frequency response functions, J. Sound Vib. 329 (2010) 3325–3334.
[43] A. Chatterjee, Nonlinear Dynamics and Damage Assessment of a Cantilever Beam With Breathing Edge Crack, J. Vib. Acoust. 133 (2011), 051004.
[44] J.K. Sinha, Higher Order Spectra for Crack and Misalignment Identification in the Shaft of a Rotating Machine, Struct. Health Monit. 6 (2007) 325–334.
[45] L. Cui, H. Xu, J. Ge, M.S. Cao, Y.M. Xu, W. Xu, D. Sumarac, Use of Bispectrum Analysis to Inspect the Non-Linear Dynamic Characteristics of Beam-Type Structures Containing a Breathing Crack, Sensors 21 (2021) 1177.
[46] J. Prawin, A.R.M. Rao, Vibration-based breathing crack identification using non-linear intermodulation components under noisy environment, Struct. Health Monit. 19 (2020) 86–104.
[47] F. Aymerich, W.J. Staszewski, Impact damage detection in composite laminates using nonlinear acoustics, Compos. A Appl. Sci. Manuf. 41 (2010) 1084–1092.
[48] A. Klepka, W.J. Staszewski, R. Jenal, M. Szwedo, J. Iwaniec, T. Uhl, Nonlinear acoustics for fatigue crack detection–experimental investigations of vibro-acoustic wave modulations, Struct. Health Monit. 11 (2012) 197–211.